Bio-physical changes in the Gulf of Mexico during the 2018 Hurricane Michael

Ebenezer S. Nyadjro, Zhankun Wang, James Reagan, Just Cebrian, and Jay F. Shriver

Abstract— **We investigate the impacts of one of the strongest recorded hurricanes to have hit the Florida Panhandle, Hurricane Michael (2018), on the upper ocean using a suite of satellite data, in-situ profiles, and outputs from the HYbrid Coordinate Ocean Model (HYCOM). Strong, low-level cyclonic winds associated with the hurricane generated strong Ekman suction that propagated ahead of the hurricane and caused changes in the surface and subsurface ocean. Following the passage of Hurricane Michael, a 3°C drop in sea surface temperature (SST) was accompanied with a 4-5 mg m^{-3} increase in chlorophyll-a concentration. In the subsurface, a ~15 m mixed layer deepening preceded upward displacements of the isotherms and cooling of the mixed layer. The impact of hurricane conditions on sea surface salinity (SSS) was localized and influenced by competing processes, with upwelling of salty subsurface water increasing SSS and enhanced precipitation decreasing SSS. During the peak of the hurricane, the impact of upwelling was greater than that of enhanced precipitation and, thus, SSS increased. Further away from the upwelling centers, hurricane-influenced precipitation, and river runoff freshened SSS.**

Index Terms— **Gulf of Mexico, Hurricane Michael, Upper ocean response, Sea surface temperature, Chlorophyll-a, Sea surface salinity.**

I. INTRODUCTION

Hurricanes interact with the ocean, with such interactions either strengthening or weakening the hurricane. Sensible and latent heat fluxes from the warm (>28°C), stratified waters of the Gulf of Mexico (GoM; Fig. 1a) makes it a suitable location for hurricane intensification [1], [2]. In turn, the hurricane feeds back to the ocean and impacts ocean thermodynamics by altering water stratification. Consequently, there is an enhancement of entrainment mixing that brings cooler waters from the subsurface ocean into the surface ocean [3]. The drop in sea surface temperature (SST), which was as high as 6 °C during hurricane Katrina [4], then contributes to weakening the intensity of the hurricanes [3], [5]. The extent of the SST drop depends on factors such as magnitude of wind forcing, ocean stratification, inertial oscillations, upwelling source depth and mixed layer thickness [3], [6], [7].

Hurricanes stimulate biological productivity. During the passage of a hurricane, strong winds generate divergent flows that cause upwelling of subsurface nutrients such as phosphate and nitrate into the euphotic, surface waters. The nutrient-rich surface waters, together with ambient light, leads to an increase in primary productivity and potentially plankton blooms days after hurricane passage. Thus, the GoM momentarily becomes more productive during the passage of hurricanes [8]. A study by [9] suggests different responses by phytoplankton groups to hurricanes in the GoM. The study found large phytoplankton to be most responsive to turbulent mixing and nutrient injection that occurred during the hurricane passage. In contrast, smaller phytoplankton could be spatially displaced, especially when advected by mesoscale eddies.
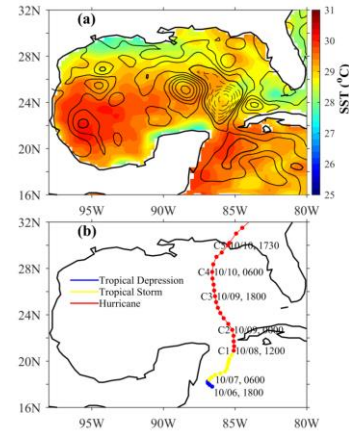

Fig.1. (a) Sea surface temperature (color shading, °C) and sea level anomaly (contours, m) during October 3, 2018. (b) Best track plot and evolution of Hurricane Michael. Times are in Coordinated Universal Time (UTC). C1-C5 stand for hurricane category 1-5.

Ocean circulation also influences the interactions between hurricanes and the upper ocean. Ocean circulation in the GoM is dominated by the Loop Current (LC), which brings in about 23-27 Sv [10] water each year. The LC sheds warm core rings (WCR) and cold core rings (CCR) that respectively strengthen or weaken hurricane intensity as the hurricane passes over them [1], [11]. Namely, WCR act as insulators against hurricane-induced upwelling and mixing, thereby reducing SST cooling and hurricane weakening. Hurricane intensification after

passing over a WCR was observed for Hurricanes Opal (1995), Bret (1999), and Katrina (2005) [11]. Conversely, CCR absorb heat from hurricanes and cause them to weaken [1], [11].

On October 10, 2018, Hurricane Michael became the first recorded category 5 hurricane to make landfall in the Florida Panhandle [12], and the first hurricane in the US to make landfall as a category 5 since Hurricane Andrew in 1992. Hurricane Michael was first noticed as a tropical disturbance at 1800 UTC on October 6 around 18°N, 86°W in the Caribbean Sea (Fig. 1b). It quickly developed into a tropical storm by 0600 UTC on October 7. By that time, the atmospheric pressure had dropped from 1006 mb to 1004 mb while its speed had increased from 25 kn to 30 kn. It continued to strengthen as it transitioned across the Gulf, becoming a category 1 hurricane by 1200 UTC on October 8 around 20.9°N, 85.1°W. It attained category 4 status by 0600 UTC on October 10 around 27.7°N, 86.6°W, at which time the pressure had dropped to 945 mb. At about 1730 UTC on October 10 Hurricane Michael attained a category five status with sustained winds of 140 kn and atmospheric pressure of 919 mb, at which time it made landfall near Mexico Beach and Tyndall Air Force Base, Florida, causing 16 deaths and property damages of about $25 billion [13]. In this letter, we examine changes in physical oceanic conditions and chlorophyll-a (chl-a) concentration in the GoM during the passage of Hurricane Michael using satellite-derived data and outputs from the HYbrid Coordinate Ocean model (HYCOM).

II. DATA AND METHODS

A. Data

Hurricane Michael best track data was obtained from the International Best Track Archive for Climate Stewardship (IBTrACS, https://www.ncdc.noaa.gov/ibtracs/). Daily SST data on a 0.25°×0.25° grid are obtained from the Advanced Very High-Resolution Radiometer (AVHRR) infrared satellite archived at the National Oceanic and Atmospheric Administration (NOAA) National Centers for Environmental Information (NCEI) [14]. Daily mean sea surface height anomaly (SSHA) data on a 0.25°×0.25° grid are obtained from Archiving, Validation, and Interpretation of Satellite data in Oceanography (AVISO) [15]. This product is produced by merging SSH from various altimetry satellites such as the European Remote Sensing Satellite (ERS-1/2), Ocean Topography Experiment (TOPEX)/Poseidon, Jason-1, Jason-2, Jason-3, Sentinel-3A, HY-2A, Saral/AltiKa, Cryosat-2, and Environmental Satellite (Envisat). The product is distributed by Copernicus Marine and Environment Monitoring Service (CMEMS) (http://www.marine.copernicus.eu).

Daily-averaged 0.25°×0.25° gridded level-3 winds are obtained from the Advanced Scatterometer (ASCAT) surface wind fields archived at the Centre de Recherche et d'Exploitation Satellitaire (CERSAT), France [16]. In this study, we used the NOAA NCEI-archived level-3 daily chlorophyll-a product produced from the Visible Infrared Imaging Radiometer Suite (VIIRS) onboard the Suomi-National Polar-orbiting Partnership (SNPP) satellite (https://www.ncei.noaa.gov/archive/accession/STAR-VIIRS-

OCR-L3). Sea surface salinity (SSS) data from the Soil Moisture Active Passive (SMAP) satellite on a 0.25°×0.25° grid are obtained from the NASA's Jet Propulsion Laboratory (JPL; https://smap.jpl.nasa.gov/data/). Daily precipitation data on a 1°×1° grid are from the University Corporation for Atmospheric Research (UCAR) Global Precipitation Climatology Product (GPCP) version 1.2 product [17].

Subsurface temperature and salinity data are obtained from the NOAA NCEI World Ocean Database [WOD; 18]. The WOD is made up of ocean profiles (e.g. from the Argo program and eXpendable Conductivity-Temperature-Depth; XCTD profiles), containing measurements of ocean variables from different depths. Information about the subsurface is supplemented with outputs (i.e. mixed layer depth, temperature, and salinity) from a reanalysis version of HYCOM. HYCOM has a horizontal resolution of 1/12° and 41 hybrid layers. The vertical coordinate is approximately equal pressure levels in the unstratified ocean and isopycnal in the open stratified ocean. The first 16 vertical layers are fixed in z-level and represent the upper 100 m [19]. It uses the NASA Goddard Institute for Space Studies (GISS) Level 2 turbulence closure mixing model. This HYCOM experiment assimilates available satellite-derived SST, and altimeter as well as in-situ salinity and temperature from Argo floats, conductivity-temperature-depth profiles, and moored buoys. HYCOM has been compared with WOD in the GoM and found to perform favorably well [20]. It has also been used to successfully study biophysical interactions during hurricane passage in the GoM [e.g. 21, 22].

B. Methods

Mixed layer depth (MLD) was computed from HYCOM using a variable density threshold equivalent to 0.2 °C [23]:

$$\Delta\sigma_\theta = \sigma_\theta(T_{10} - 0.2, S_{10}, P_0) - \sigma_\theta(T_{10}, S_{10}, P_0) \quad (1)$$

where $\Delta\sigma_\theta$ is the change in potential density between the reference depth (10 dbar) and the base of the mixed layer. T_{10} and S_{10} are respectively temperature and salinity at 10 dbar, and P_0 is sea surface pressure.

Ekman suction velocity (w_e) was computed from:

$$w_e = \frac{1}{\rho_o f} \nabla \times \boldsymbol{\tau} \quad (2)$$

where $\nabla \times \boldsymbol{\tau}$ is the curl of the derived wind stress vector, ρ_o is the density of seawater (1024 kg m^{-3}), f is the Coriolis parameter (2Ωsinφ, where Ω is the angular velocity of the Earth and φ is the latitude).

III. RESULTS AND DISCUSSION

A. Temperature changes

Prior to the occurrence of Hurricane Michael, SST in the GoM was warm (>28°C), making the basin susceptible to cyclogenesis (Fig. 1a). SST is essential for hurricanes by supplying moist enthalpy via heat fluxes which leads to intensification of the hurricane [2], [5]. With the importance of excessive heat content to the formation and sustenance of

hurricanes, the GoM becomes a fertile ground for intensification. During the passage of a hurricane, the strong winds associated with the hurricane force sea surface cooling via evaporative surface flux, mixing, entrainment, and upwelling [3], [6]. Daily SST tendency (i.e. $\partial SST/\partial t$; where t is time) during the passage of Hurricane Michael are shown in Fig. 2. Overall, there was an SST cooling of ~3°C from the hurricane formation to its demise. The extent of SST cooling is concomitant with hurricane intensity (i.e. low hurricane central pressure). Also, low hurricane translational speed causes a greater change in SST [5]. Prior to the emergence of Hurricane Michael, SST was relatively stable in the GoM (Fig. 2a). By October 7, SST tendency shows a cooling of about 1°C day^{-1} centered on 86°W, 20°N, where the hurricane sits in the GoM. This cooling then intensified and became more widespread in the open ocean during October 8-9 (Fig. 2c, d). The maximum SST cooling in the open ocean occurred over pre-existing cyclonic circulation and associated Ekman suction (i.e. negative SLA; Fig. 2c-e). Prior to the passage of Hurricane Michael, a cyclonic circulation centered at 86°W, 24°N had formed (Fig. 1a). The strong hurricane winds caused this cyclonic circulation to intensify as SLA depressions exceeding 10 cm occurred over the duration of the hurricane. As Hurricane Michael passes over this cyclonic circulation feature, it induced further cooling (Fig.1a, Fig. 2).

As Hurricane Michael peaked and eventually made landfall in the northern GoM during 9-10 October, the SST cooled by over 1.5 °C day^{-1} along the coastal region, with the coldest SST occurring to the right of the hurricane path (Fig. 2d, e). These satellite data-derived SST changes during the transition of Hurricane Michael are confirmed by the WOD profiles in the northeastern GoM (Fig. 3a). The asymmetric cooling along the hurricane track (Fig. 2) is consistent with previous occurrences and can be attributed to the winds being strongest on that side of the hurricane track [3], [6], [24]. In addition, the wind stress is counterclockwise and enables strong surface divergence and upwelling to occur. By October 11 (Fig. 2f), after the hurricane had made landfall near Mexico Beach and Tyndall Air Force Base, Florida, SST in the GoM showed a tendency to rebound to a warming state.
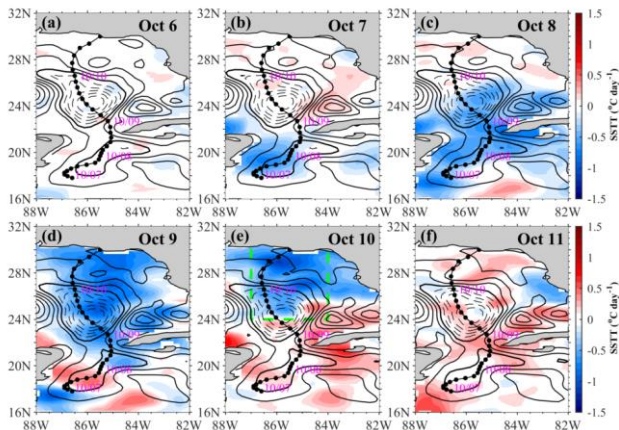

Fig.2. Sea surface temperature tendency (SSTT; color shading, °C day^{-1}) and sea level anomaly (contours, m) during October 6-11, 2018. Overlaid is Hurricane Michael's best track. Green box marks the box-averaging region (24ºN-30ºN, 84ºW-87ºW).
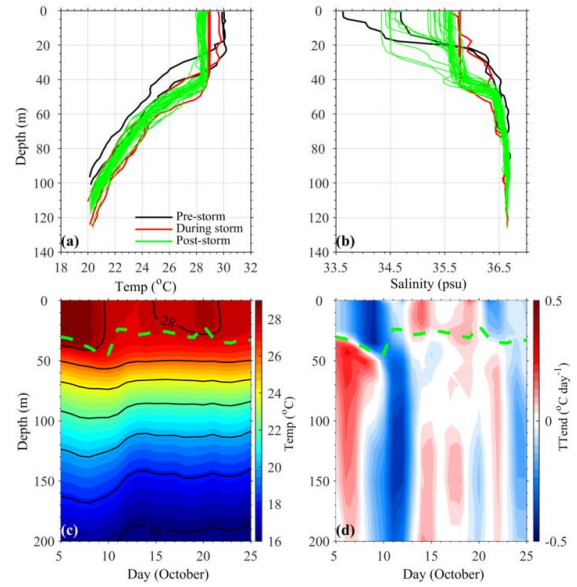

Fig.3. (a) Temperature (ºC) and (b) salinity (psu) plots from the World Ocean Database profiles in the northeastern Gulf of Mexico (28ºN-30ºN, 85ºW-88ºW) before (9/27/2018-10/5/2018), during (10/6/2018-10/10/2018) and after (10/11/2018-10/20/2018) the passage of Hurricane Michael. Time-depth plots of HYCOM (c) temperature (color shading and black contour, ºC), and (d) temperature tendency (color shading, ºC day^{-1}) in the upper 200 m. Mixed layer depth from HYCOM (green line, m), box-averaged over green box region in Fig. 2e (24ºN-30ºN, 84ºW-87ºW) is overlaid in Fig. 3c and 3d.

B. Chlorophyll-a changes

A noticeable feature during hurricanes is the increase in chl-a concentrations [6], [8], [9]. Factors that determine the magnitude of chl-a changes in surface waters include hurricane translational speed, upwelling-source depth, rapid breakdown of stratification, and increased precipitation which increases the transport of terrigenous nutrients into the coastal waters [4], [6], [25]. The distributions of chl-a during the passage of Hurricane Michael are presented in Fig. 4, with highest concentrations along the coastal waters. There is chl-a enhancement (Fig. 2) associated with the SST cooling in the coastal area (Fig. 4). During September 30-October 7, mean chl-a concentration in the coastal northeastern GoM was ~1.52 mg m^{-3}. This increased to ~2.2 mg m^{-3} during October 8-15, a period covering the peak of the hurricane and after it made landfall. During October 16-23, a week after the hurricane passage, mean chl-a reduced marginally to ~1.96 mg m^{-3}, but still higher than before the hurricane passage (Fig. 4c). A study by [4] suggests that chl-a enrichments during hurricane passages in the GoM are often from both new production resulting from nutrient entrainment as well as from chl-a entrained from the subsurface ocean into the surface ocean.
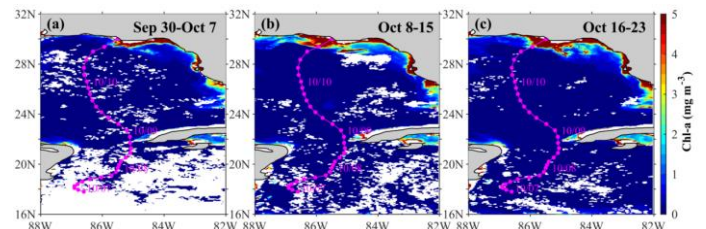

Fig.4. Weekly averaged chl-a concentrations (mg m^{-3}). Overlaid is Hurricane Michael's best track.

C. Salinity changes

The impact of Hurricane Michael on SSS in coastal northern GoM is shown in Fig. 3b and Fig. 5. There are localized responses of the SSS to hurricane-influenced conditions. SSS along the path of the hurricane increased during the peak and immediately following the passage of the hurricane (Fig. 3b, 5e, 5f). Although there was a high amount of precipitation at the peak of the hurricane (>60 mm day^{-1}; Fig. 5b), it did not freshen SSS along its path. Indeed, the blob of freshwater centered around 88°W, 28°N observed on October 3 (Fig. 5d) had waned and become saltier during October 10 and October 17. This local salinification can be attributed to the vertical advection of high salinity subsurface waters as part of the enhanced upwelling that occurred in the area (i.e. see Fig. 6e), which overwhelms the impact from precipitation. Conversely, further west of the local upwelling region, between 90°W and 95°W, the fresh coastal water observed during October 3 became fresher during October 10 and October 17 (Fig. 5), most likely from the impacts of precipitation and runoff.
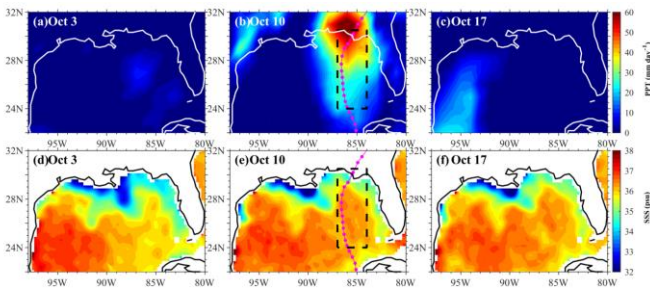

Fig.5. Precipitation (upper row, mm day^{-1}) and sea surface salinity (lower row, psu) before (left column), during (middle column) and after (right column) the passage of Hurricane Michael.

D. Subsurface changes

The regions of strong surface cooling (Fig. 2, 3) coincide with the regions of strong Ekman suction velocity (Fig. 6), suggesting the cool subsurface waters (Fig. 3) to be a source of the cold surface waters. Indeed, upwelling has been identified as an important process that displaces isotherms and changes the water density in the mixed layer during the passage of hurricanes in the GoM [5], [6], [8]. Upwelling, while enhancing primary productivity, also causes SST to reduce significantly which subsequently feeds back to weaken the hurricane. We note a significant increase in Ekman suction along the path of Hurricane Michael as it makes its way towards the northern GoM coast (Fig. 6). Low-level cyclonic winds associated with the hurricane generate this strong Ekman suction.

Prior to upwelling contributing to surface cooling, the strong, hurricane winds first cause evaporative cooling. During the passage of Hurricane Michael, total heat flux from HYCOM changed from -100 Wm^{-2} on October 5 to about -350 Wm^{-2} at the peak of the hurricane (Figure not shown). As the surface layer cools, and the subsurface warms (possibly from density compensation; Fig. 3d; [2], [26]), the water stratification wanes, creating an instability and making the water column susceptible to mixing [2], [27]. The mixed layer depth deepens accordingly by ~15 m (Fig. 3) and leads the cooling of subsurface

temperature by about two days. Post-mixed layer deepening, the isotherms shoal upward, signifying possible entrainment of cooler deeper waters into the thermocline and mixed layer which leads to cooling of the mixed layer. After the hurricane landfall, the entire water column is cooled with the most cooling occurring in the thermocline area. By October 14, the cooling tendency in the upper 200 m had waned, with the tendency for warming observed (Fig. 3d). The shallow, warm, quasi-permanent stratified nature of the GoM enables it to rebound swiftly after the passage of Hurricane Michael, reestablishing stability of the water column [4].

Hurricane Michael-induced upwelling caused a thermocline displacement of 20 m (Fig. 3). As the hurricane formed in the Caribbean Sea, Ekman suction was relatively weak, 0.5-1 4×10^{-4} ms^{-1} and occurred to the right of the hurricane track (Fig. 6a). Afterwards, Ekman suction increased along the path of the hurricane and at its peak, Ekman suction was about 4×10^{-4} ms^{-1}. The relatively strong upwelling results from strengthening of the wind stress curl as the hurricane intensifies which causes greater divergence of the water column and injection of cold, subsurface waters into the surface ocean. An interesting feature to note is that Ekman suction occurs and propagates ahead of the path of the hurricane. For example during October 8 (Fig. 6c) while the hurricane sits near 85°W, 21°N there is a strong Ekman suction of ~4×10^{-4} ms^{-1} occurring at 85.5°W, 23°N. By October 11, after the passage of Hurricane Michael over the GoM, Ekman suction was virtually null in the entire basin as the cyclonic winds had waned (Fig. 6f).
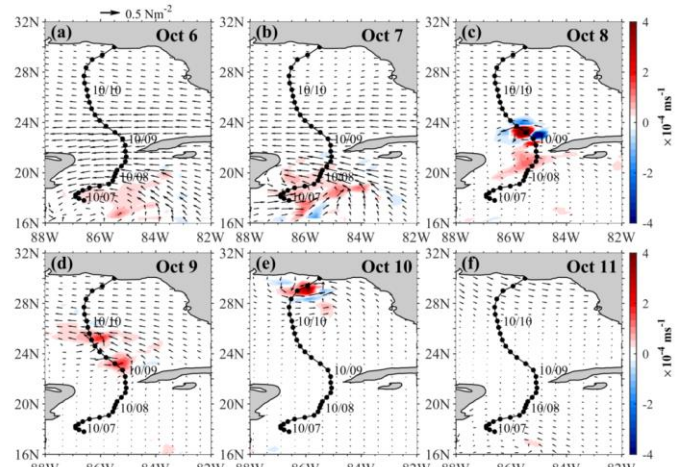

Fig.6. Ekman suction velocity (color shading, ms^{-1}) and wind stress (vectors, Nm^{-2}) during October 6-11, 2018. Overlaid is Hurricane Michael's best track.

IV. SUMMARY AND CONCLUSION

Hurricane Michael was the first recorded category 5 hurricane to make landfall in the Florida Panhandle, causing deaths and extensive destruction of properties. As it formed in the Caribbean Sea on October 6, 2018, and transitioned across the GoM, it interacted with the ocean and caused changes in surface and subsurface ocean properties. We used satellite-derived data, WOD profiles, and HYCOM outputs to describe the bio-physical changes that occurred in the GoM during the passage of Hurricane Michael. Strong SST cooling occurred

along the path of the hurricane. The cooling was caused by upwelling driven by intense Ekman suction that resulted from intensification of low-level cyclonic winds, consistent with previous studies [e.g. 3, 4, 6, 25]. Mixed layer deepening preceded upward displacements of the isotherms and cooling of the mixed layer. Maximum SST cooling in the open ocean occurred over pre-existing cyclonic circulation. Namely, as the hurricane passed over areas with pre-existing cyclonic circulation, the already uplifted thermocline and weak stratification allowed for an easier entrainment of colder subsurface waters into the upper ocean. Venting of the thermocline by upwelling and inputs of terrigenous nutrients by intense precipitation, both caused by the hurricane, caused chl-a enrichment in the coastal area. The injection of cold, salty subsurface waters into the surface ocean overwhelmed the increased precipitation from the hurricane. Further away from the regions of coastal upwelling, however, SSS freshened likely from hurricane precipitation and increased river runoff. A complete salt budget estimation from modelling studies will enable a comprehensive understanding of these processes.

REFERENCES

[1] L. K. Shay, G. J. Goni, and P. G. Black, "Effects of a warm oceanic feature on Hurricane Opal," Mon. Weather Rev., vol. 128, no. 5, pp. 1366–1383, May 2000.
[2] B. Dzwonkowski, J. Coogan, S. Fournier, G. Lockridge, K. Park, and T. Lee, "Compounding impact of severe weather events fuels marine heatwave in the coastal ocean," Nat. Commun., vol. 11, Sep. 2020, Art. no. 4623.
[3] J. F. Price, "Upper ocean response to a hurricane," J. Phys. Oceanogr. Vol. 11, pp. 153–175, Feb. 1981.
[4] M. M. Gierach, and B. Subrahmanyam, "Biophysical responses of the upper ocean to major Gulf of Mexico hurricanes in 2005," J. Geophys. Res., vol. 113, no. C4, pp. 1–11, Apr. 2008, Art. no. C04029.
[5] K. A. Emanuel, "Thermodynamic control of hurricane intensity," Nature, vol. 401, no. 6754, pp. 665–669, Oct. 1999.
[6] N. D. Walker, R. R. Leben, and S. Balasubramanian, "Hurricane-forced upwelling and chlorophyll a enhancement within cold-core cyclones in the Gulf of Mexico," Geophys. Res. Lett., vol. 32, Sep. 2005, Art. no. L18610.
[7] Z. Wang, S. F. DiMarco, M. M. Stossel, X. Zhang, M. K. Howard, K. du Vall, "Oscillation responses to tropical Cyclone Gonu in northern Arabian Sea from a moored observing system," Deep-Sea Res Pt I, vol. 64, pp. 129–145, Mar. 2012.

[8] S. M. Babin, J. A. Carton, T. D. Dickey, and J. D. Wiggert, "Satellite evidence of hurricane-induced phytoplankton blooms in an oceanic desert," J. Geophys. Res., vol. 109, Mar. 2004. Art. no. C03043.
[9] M. M. Gierach, B. Subrahmanyam, A. Samuelsen, and K. Ueyoshi, "Hurricane-driven alteration in plankton community size structure in the Gulf of Mexico: A modeling study," Geophys. Res. Lett., vol. 36, Apr. 2009, Art. no. L07604.
[10] J. Sheinbaum, J. Candela, A. Badan, and J. Ochoa, "Flow structure and transport in the Yucatan Channel," Geophys. Res. Lett., vol. 29, no. 3, pp. 10-1–10-4, Feb. 2002.
[11] X. Hong, S. W. Chang, S. Raman, L. K. Shay, and R. Hodur, "The interaction between Hurricane Opal (1995) and a warm core ring in the Gulf of Mexico," Mon. Weather Rev., vol. 128, no. 5, pp. 1347–1365, May 2000.
[12] N. E. Zampieri, S. Pau, and D. K. Okamoto, "The impacts of Hurricane Michael on longleaf pine habitats in Florida," Nat. Commun, vol. 10, May 2020, Art. no. 8483.
[13] J. Bevan II, R. Berg, and A. Hagen, "National Hurricane Center Tropical Cyclone Report: Hurricane Michael (AL142018) 7–11 October 2018," National Hurricane Center, https://www.nhc.noaa.gov/data/tcr/AL142018_Michael.pdf , 2019.
[14] R. W. Reynolds, T. M. Smith, C. Liu, D. B. Chelton, K. S. Casey, and M. G. Schlax, "Daily High-Resolution-Blended Analyses for Sea Surface Temperature," J. Clim. Vol. 20, pp. 5473-5496, Nov. 2007.
[15] N. Ducet, P-Y. Le Traon, and F. Reverdin, "Global high-resolution mapping of ocean circulation from TOPEX/Poseidon and ERS-1/2," J. Geophys. Res., vol. 105, no. C8, pp. 19,477–19,498, Aug. 2000.
[16] A. Bentamy, and D. Croize-Fillon, "Gridded surface wind fields from Metop/ASCAT measurements," Int. J. Remote Sens., vol. 33, no. 6, pp. 1729-1754, Mar. 2012.
[17] G. J. Huffman, R. F. Adler, M. M. Morrissey, D. T. Bolvin, S. Curtis, R. Joyce, B. McGavock, and J. Susskind, "Global precipitation at one-degree daily resolution from multi-satellite observations," J. Hydrometeor., vol. 2, pp. 36-50, Feb. 2001.
[18] T. P. Boyer, O. K. Baranova, C. Coleman, H. E. Garcia, A. Grodsky, R. A. Locarnini, A. V. Mishonov, C. R. Paver, J. R. Reagan, D. Seidov, I.V. Smolyar, K.W. Weathers, M. M. Zweng. "World Ocean Database 2018". A. V. Mishonov, Technical Editor, NOAA Atlas NESDIS 87, 2018.
[19] E. J. Metzger, R. W. Helber, P. J. Hogan, P. G. Posey, P. G. Thoppil, T. L. Townsend, et al., "Global Ocean Forecast System 3.1 validation testing," Naval Research Laboratory Technical Report. Retrieved from http://www.dtic.mil/docs/citations/AD1034517. 2017.
[20] C. A. Cleveland, "Empirical Validation and Comparison of the Hybrid Coordinate Ocean Model (HYCOM) Between the Gulf of Mexico and the Tongue of the Ocean," Master's thesis. Nova Southeastern University. https://nsuworks.nova.edu/occ_stuetd/499. 2018.
[21] T. G. Prasad, and P. J. Hogan, "Upper-ocean response to Hurricane Ivan in a 1/25° nested Gulf of Mexico HYCOM," J. Geophys. Res., vol. 112, Apr. 2007, Art. no. C04013.
[22] M.M. Gierach, B. Subrahmanyam, and P.G. Thoppil, "Physical and Biological Responses to Hurricane Katrina (2005) in a 1/25° nested Gulf of Mexico HYCOM," J. Mar. Sys., vol 78, no. 1, pp. 168-179, Aug. 2009.
[23] C. de Boyer Montégut, G. Madec, A. S. Fischer, A. Lazar, and D. Iudicone, "Mixed layer depth over the global ocean: An examination of profile data and a profile-based climatology," J. Geophys. Res., vol. 109, no. C4, pp. 1-20, Dec. 2004, Art. no. C12003.
[24] L. J. Spencer, S. F. DiMarco, Z. Wang, J. J. Kuehl, and D. A. Brooks, "Asymmetric oceanic response to a hurricane: Deep water observations during Hurricane Isaac," J. Geophys. Res. Oceans, vol. 121, pp. 7619–7649, Jul. 2016.
[25] C. B. Trott, and B. Subrahmanyam, "Satellite Data Analysis of the Upper Ocean Response to Hurricane Dorian (2019) in the North Atlantic Ocean," IEEE Geosci. Remote Sens. Lett. 10.1109/LGRS.2020.3032062, 2020.
[26] G. Spiro Jaeger, and A. Mahadevan, "Submesoscale-selective compensation of fronts in a salinity-stratified ocean," Sci. Adv. 4, e1701504, Feb. 2018.
[27] S. Li, C. Chen, Z. Wu, R. C. Beardsley, and M. Li, "Impacts of oceanic mixed layer on hurricanes: A simulation experiment with Hurricane Sandy," J. Geophys. Res., vol. 125, no. 11, Oct. 2020.